

FRAGMENT OF THE SUPPORT STRUCTURE OF AN ENGINE VHS-404 – GREY CAST IRON – MODERN TIMES – SWITZERLAND

Artefact name Fragment of the support structure of an engine VHS-404

Authors Marianne. Senn (EMPA, Dübendorf, Zurich, Switzerland) & Christian. Degriigny (HE-Arc CR, Neuchâtel, Neuchâtel, Switzerland)

Url /artefacts/1570/

∨ The object



Credit HE-Arc CR.



Fig. 1: Fragment (left) of the painted support structure of the engine from the SS Rigi steamer (right) (after www.verkehrshaus.ch, consulted on December 5, 2011),

∨ Description and visual observation

| | |
|--|---|
| Description of the artefact | Corroded fragment (Fig. 1) of the painted support structure of the engine from the SS Rigi steamer. |
| Type of artefact | Supporting structure |
| Origin | Flush-deck side-wheel paddle steamer SS Rigi, Luzern, Lucerne, Switzerland |
| Recovering date | Removed in 1952 during the last renovation |
| Chronology category | Modern Times |
| chronology tpq | <input type="text" value="1860"/> A.D. ▼ |
| chronology taq | <input type="text" value="1896"/> A.D. ▼ |
| Chronology comment | Cast by Escher Wyss |
| Burial conditions / environment | Outdoor to indoor atmosphere |
| Artefact location | Swiss Museum of Transport, Luzern, Lucerne |
| Owner | Swiss Museum of Transport, Luzern, Lucerne |
| Inv. number | VHS-404 |
| Recorded conservation data | Renovated in 1860 and 1880. The engine was replaced in 1894 and in 1952. |

Complementary information

SS Rigi steamer is the oldest surviving flush-deck side-wheel paddle steamer in the world.

Study area(s)

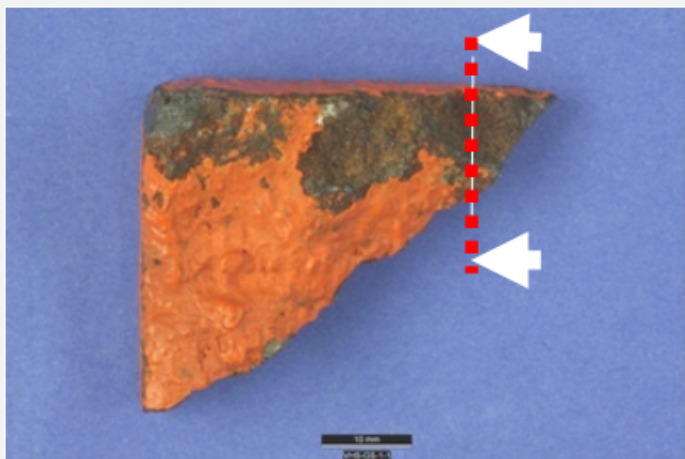


Fig. 2: Location of sampling area,

Credit HE-Arc CR.

Binocular observation and representation of the corrosion structure

None.

MiCorr stratigraphy(ies) – Bi

Sample(s)

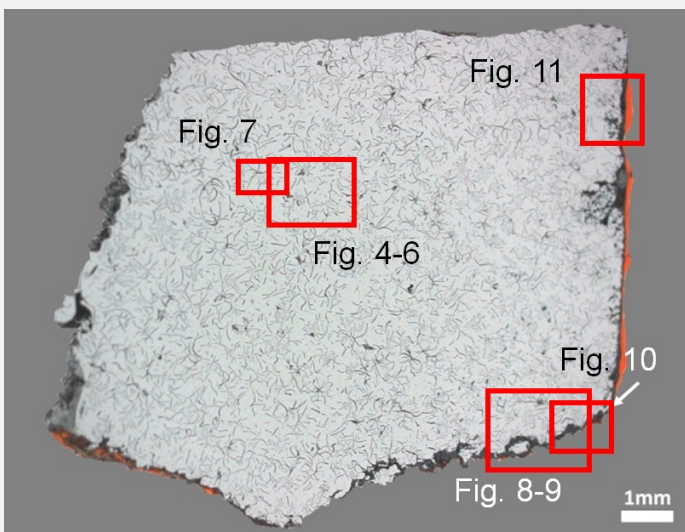


Fig. 3: Micrograph of the cross-section of the fragment showing the location of Figs. 4 to 11,

Credit HE-Arc CR.

| | |
|---------------------------------|---|
| Description of sample | The sample is a cross-section through the fragment of the support structure of the engine (Fig. 3). Dimensions: Lmax = 10mm; Wmax = 10mm. |
| Alloy | Grey cast iron |
| Technology | As-cast |
| Lab number of sample | VHS-G-1 |
| Sample location | HE-Arc CR, Neuchâtel, Neuchâtel |
| Responsible institution | Swiss Museum of Transport, Luzern, Lucerne |
| Date and aim of sampling | 07/09/2009 metallography |

Complementary information

None.

Analyses and results

Analyses performed:

Metallography (nital etched), Vickers hardness testing, LA-ICP-MS, SEM/EDS.

Non invasive analysis

None.

Metal

The remaining metal is a high P and Si grey cast iron with elevated Mn and V contents (Tables 1 and 2). The structure contains black graphite flakes and graphite nodules (Fig. 4) as well as angular grey manganese sulphide inclusions which can contain a dark alumina-rich centre (Fig. 4 and Table 1). The graphite flakes are irregular and vary in size. At low magnification the flakes are evenly spread over the entire surface with a tendency to form clusters. Some porosity is noticeable. Under SEM, in the BSD-mode, an additional eutectic phase is visible (Fig. 5). After etching one can see how the graphite is surrounded by alpha-iron in a pearlite matrix (Figs. 6 and 7). The lamellar pearlite includes steadite (Fe₃P) and manganese sulphide (MnS) inclusions. According to the cast iron diagram after Maurer (Bargel and Schulze 2008, 257), the structure is typical for a hypoeutectic pearlitic grey cast iron (C content <4.3 mass%, Si content ca. 2.0 mass%) including pearlite, steadite and graphite. The slow cooling rate and the higher Si level have favoured the formation of graphite. The high P content favours the growth of interconnected networks of steadite. The average hardness of the metal is HV1 160. This hardness is only approximate. Normally cast iron hardness is determined with a Brinell test, but due to the small size of the sample this could not be carried out. The calculated HB is about 150.

| Elements | Ni/Co | Al | P | Ti | V | Cr | Mn | Co | Ni | Cu | As | Mo | Ag | Sn | Sb | W | C* mass% |
|-----------------------|-------|----|-------|------|------|-----|------|-----|-----|-----|-----|----|----|-----|----|---|----------|
| Median mg/kg | 2.9 | < | 20000 | 1200 | 2000 | 700 | 4500 | 160 | 460 | 110 | 610 | 20 | < | 10 | 20 | < | <4.3 |
| Detection limit mg/kg | - | 4 | 73 | 8 | 1 | 11 | 2 | 1 | 3 | 1 | 2 | 3 | 1 | 0.4 | 1 | 2 | - |
| RSD % | 2 | - | 47 | 26 | 38 | 19 | 18 | 3 | 2 | 10 | 14 | 30 | - | 17 | 13 | - | - |

*visually estimated

Table 1: Chemical composition of the metal (<: below the detection limit). Method of analysis: LA-ICP-MS, Lab Inorganic Chemistry, ETH.

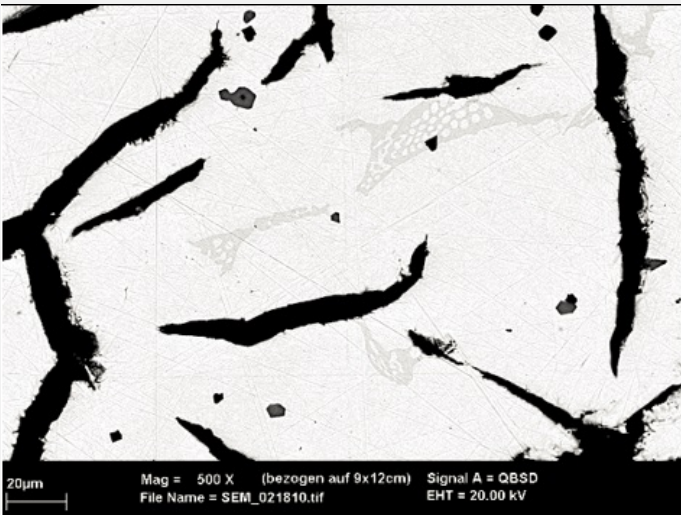
| Elements | O | Al | Si | P | S | Ti | Mn | Fe | Total |
|--|----|----|----|----|----|----|----|----|-------|
| MnS inclusions (centre) | 23 | 21 | 20 | < | < | 6 | 30 | 2 | 102 |
| MnS (global) | < | < | < | < | 35 | < | 60 | 2 | 98 |
| Metal (average of 5 similar analyses) | < | < | 2 | 2 | < | < | <1 | 95 | 100 |
| Steadite (Fe ₃ P) (average of 3 similar analyses) | < | < | < | 16 | < | < | 1 | 88 | 105 |

Table 2: Chemical composition (mass %) of the metal (<: below the detection limit). Method of analysis: SEM/EDS, Laboratory of Analytical Chemistry, Empa.



Credit HE-Arc CR.

Fig. 4: Micrograph of the metal sample from Fig. 3 (inverted picture, detail), unetched, bright field. We observe graphite flakes and irregular nodules in black and the metal in white. The small grey spots are manganese sulphide inclusions,



Credit HE-Arc CR.

Fig. 5: SEM image from Fig. 3 (detail), BSE-mode, unetched. We observe the graphite flakes in black, the manganese sulphide inclusions in grey and the eutectic mixture in light-grey,

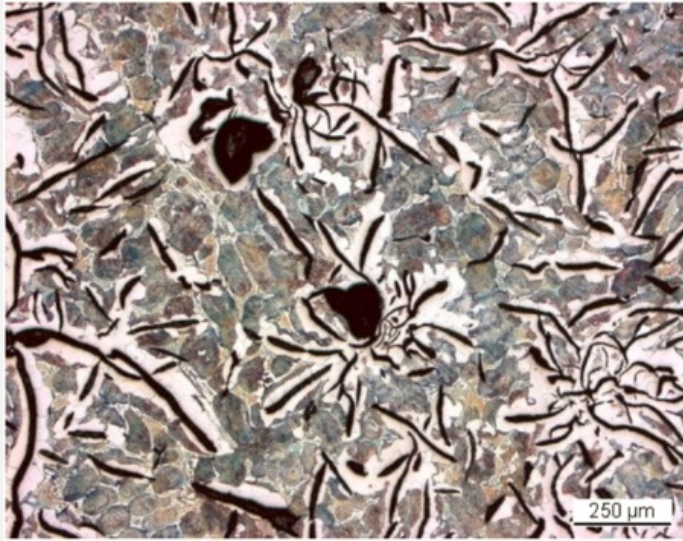


Fig. 6: Micrograph (same as Fig. 4), etched, bright field. In between the black graphite flakes we observe alpha-iron in white and pearlite / steadite in grey,

Credit HE-Arc CR.

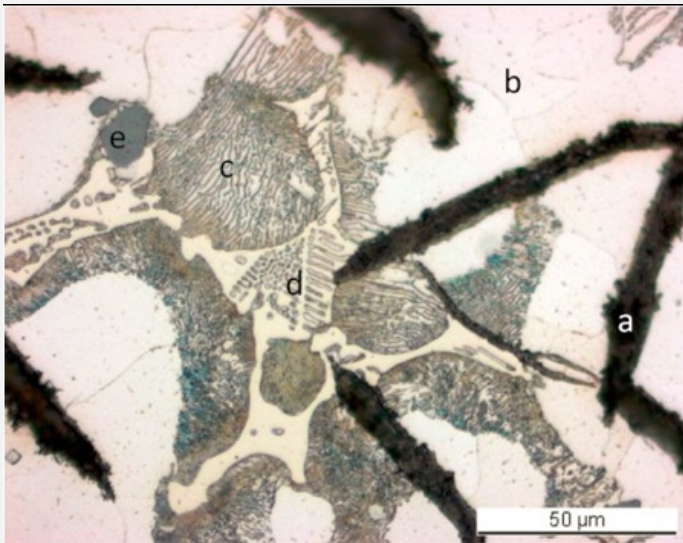


Fig. 7: Micrograph of the metal sample from Fig. 3 (detail), etched, bright field. The structure is composed of graphite (a), ferrite (b), pearlite (c), steadite (d) and MnS inclusions (e),

Credit HE-Arc CR.

| | |
|-----------------------------|---|
| Microstructure | Graphite lamellars + pearlite + ferrite + steadite (Fe3P) |
| First metal element | Fe |
| Other metal elements | C, Si, P, Ti, V, Mn |

Complementary information

None.

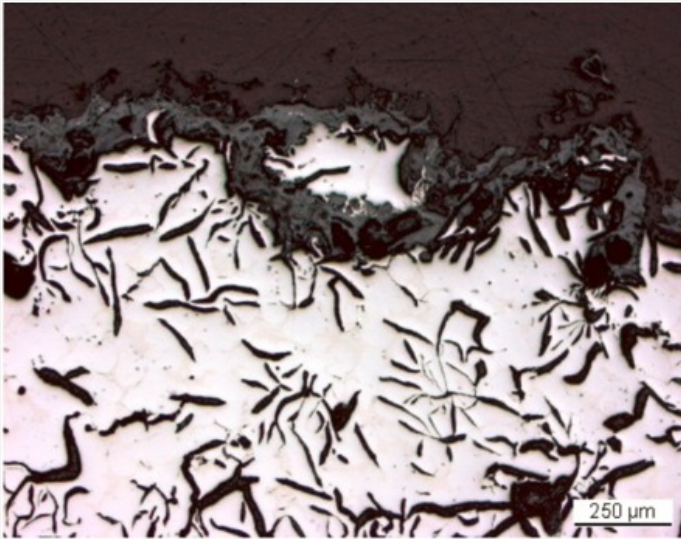
Corrosion layers

The thin corrosion crust (CP1) is limited to three sides of the sample and some remains of a paint coating (orange) are visible (Fig. 3). In bright field, the corrosion crust appears light-grey (Fig. 8), under polarised orange (Fig. 9). It is mainly composed of iron oxides (Table 3 and Fig. 10). The Pb and Ba-rich paint system has been applied directly onto the oxidized Fe, Si and Mn-rich casting skin (Fig. 11). The paint layer is probably an anodic inhibitor made from minium (red lead) with a barium sulphate filler. Because of the interference of Pb with S in the EDS spectra S is difficult to detect.

| Elements | O | Mg | Si | P | S | Mn | Fe | Ba | Pb | Total |
|--|----|----|----|---|---|----|----|----|----|-------|
| Inner light-grey corrosion layer (Fig. 11) | 20 | < | < | < | < | 1 | 76 | < | < | 97 |

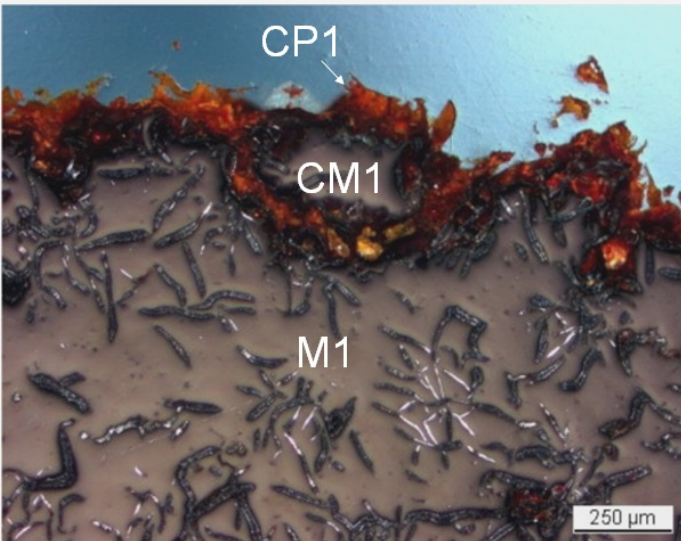
| | | | | | | | | | | |
|----------------------------------|----|---|----|---|----|----|----|----|----|----|
| Dark-grey casting skin (Fig. 11) | 27 | < | 14 | < | < | 21 | 33 | < | < | 95 |
| Paint system (Fig. 11) | 20 | < | < | < | < | < | < | 18 | 55 | 93 |
| Grey corrosion layer (Fig. 10) | 35 | < | 1 | < | <1 | < | 59 | < | < | 96 |

Table 3: Chemical composition (mass %, <: below the detection limit) of the corrosion layer (from Figs. 10 and 11). Method of analysis: SEM/EDS, Laboratory of Analytical Chemistry, Empa.



Credit HE-Arc CR.

Fig. 8: Micrograph showing the metal - corrosion layer interface from Fig. 3 (inverted picture, detail), unetched, bright field. We observe in white the metal, in light-grey the corrosion layer, in black the graphite flakes,



Credit HE-Arc CR.

Fig. 9: Micrograph (same as Fig. 8) corresponding to the stratigraphy of Fig. 12, unetched, polarised light. We observe in violet the metal, in orange the corrosion, in blue the resin,

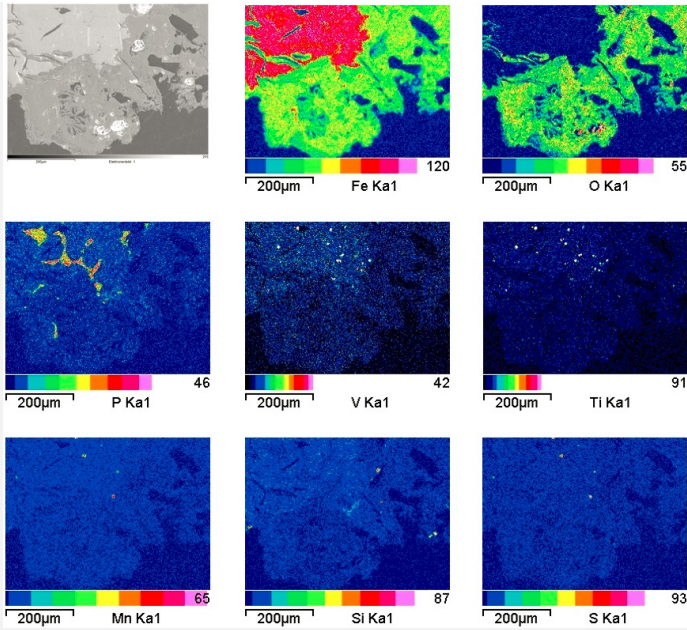


Fig. 10: SEM image, SE-mode, and elemental chemical distribution of the selected area from Fig. 3 (detail). Method of examination: SEM/EDS, Laboratory of Analytical Chemistry, Empa,

Credit Empa.

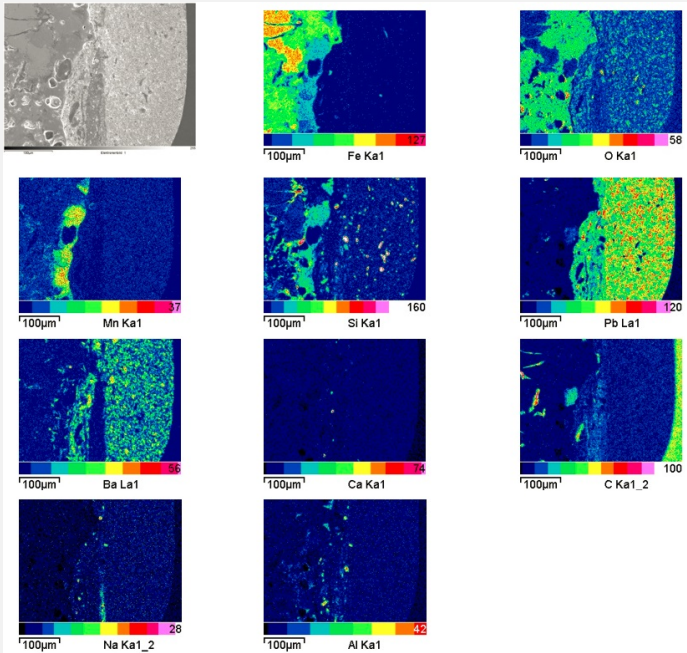


Fig. 11: SEM image, SE-mode, and elemental chemical distribution of the selected area from Fig. 3 (detail). Method of examination: SEM/EDS, Laboratory of Analytical Chemistry, Empa,

Credit Empa.

Corrosion form Uniform - transgranular

Corrosion type Unknown

Complementary information

None.

⌵ MiCorr stratigraphy(ies) – CS

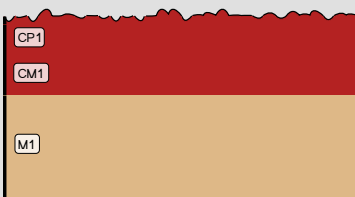


Fig. 12: Stratigraphic representation of an unpainted section of the fragment in cross-section (dark field) using the MiCorr application. The characteristics of the strata are only accessible by clicking on the drawing that redirects you to the search tool by stratigraphy representation. This representation can be compared to Fig. 10, Credit HE-Arc CR.

✧ Synthesis of the binocular / cross-section examination of the corrosion structure

None.

✧ Conclusion

The metal is a hypoeutectic pearlitic grey cast iron with significant amounts of Si and P. A P-content in excess of 0.4 mass % causes a decrease in the tensile and impact strength. P is concentrated in the hard, brittle steadite phase. Supporting elements for machines are often manufactured from such metal because it can absorb a high degree of vibration. The metal is still covered by the casting skin which was left as a natural protection against corrosion. A Pb-based anodic paint system formed a further protection layer. The corrosion is minimal.

✧ References

References on object and sample

References object

1. Auskunftsblatt der Sammlung des Verkehrshauses der Schweiz Luzern (Wasserverkehr) zu VHS-404.

References sample

2. Senn, M (2011) Prüfbericht 205'340-2.

References on analytic methods and interpretation

3. Bargel, H-J., Schulze, G. (ed.) (2008) Werkstoffkunde, Springer, 249-270.